Power System Topology Proposal of a High-Altitude Pseudo-Satellite: Sizing Method, Power Budget Modeling and Efficient Power Control

Abderrahmane SEDDJAR, Kamel Djamel Eddine KERROUCHE, Nassima KHORCHEF
Algerian Space Agency, Algeria
aseddjar@cds.asal.dz

***Abstract*—In aerospace research, the High-Altitude Stratospheric Platform System (HAPS), is becoming an effective alternative solution to perform Earth observation missions, where several problems faced by aircraft systems can be solved. The most important advantages of HAPSs are their manufacturing and launch cost reduction compared to the satellites, with enough durability to provide services as satellites do. For a successful HAPS mission, it is imperative to assess the feasibility of their deployment in a given location, where, the energy generation and consumption are the main constraints. Therefore, the conception of an Electrical Power System (EPS) has been considered as a fundamental issue in HAPS development. In this paper, a proposed EPS topology, for HAPS dedicated to Earth observation missions, is presented with a proposed sizing method, power budget modeling, and a novel efficient power control based on fuzzy logic approach.**

***Index Terms*—aerospace engineering, aerospace electronics, earth observing system, fuzzy control, power system control.**

I. INTRODUCTION

High-Altitude Pseudo-Satellites (HAPS) are those aerospace platforms able to compete with satellite operations and performances [1-6], which means enough altitude (20 to 50 km) for the payloads to cover an interesting area without interfering with current commercial aviation, and have a sufficient endurance to provide different services [7,8]. They can, in addition, provide high-resolution payloads data that complement geostationary and polar-orbiting spacecraft missions [3].

As costs are time-dependent and there is a lot of progress in cost-effective communications technologies and advances in solar panel efficiency, lightweight composite materials, autonomous avionics, and antennas, HAPS are becoming more economically feasible in the future. HAPS missions can be either military or civil; their purposes are considered for many applications such as maritime and border observations, telecommunications, missile detection, environmental monitoring, etc. Currently, both aerostatic and aerodynamic solutions are in the race for stratospheric conquest [1], [9]. HAPSs are expected to offer advantages and complementary applications over space and terrestrial platforms and to exhibit the best features.

For continuous operations throughout the desired HAPS mission duration, the energy requirements of all on-board subsystems define how much energy is needed to maintain flight to support the payload using solar panels as a primary energy source during the daylight and batteries to store the rest of the produced energy for night-time operations. The harvested energy depends on many factors such as the solar irradiance, the daylight duration, the HAPS attitude, the solar panels, and batteries performances etc.; this requires an adequate Electrical Power System (EPS) architecture and consumption modeling for both the platform and the payloads.

While many research [10-13] studied the design and performance of solar-powered aircraft, most focus on aerodynamical and mechanical issues. Only a few studies [14-16] consider solar cell energy harvesting and managing problems. In [17-19], authors focused on the solar energy and electrical systems performances at high altitudes; considering the most significant energy-consuming subsystems, they suggest that only solar cells at high altitudes can potentially provide enough energy to support an aircraft. A stratospheric photovoltaic solar model is developed in [15]; the model originally considers that the aircraft is at the ground level then adjusted for stratospheric altitude, thus, an energy collection model based on stratospheric radiation suitable for the aircraft applications is required. However, this work also requires a comparison between the harvested energy and the total consumed. Conversely, in [20], the analysis of a hybrid solar high-altitude long-endurance unmanned aerial vehicle is presented; where, the methodology minimizes the energy consumption of the aerial platform considering the energy balance for a climb, cruise, and landing cycles, respectively. In [21], the energy management of solar-powered aircraft-based high-altitude platforms for wireless communications is given; in this study, the energy harvesting model is presented considering the total movement from sunrise to sunset. However, the aerodynamic shape of the wings is not considered, this can influence the precision of the obtained results.

The research presented within this paper investigates the areas relating to HAPS's EPS, where, the EPS architecture, power sources sizing techniques, power budget modeling, and a novel power control method are presented. This work aims to spot-out the challenges associated particularly with the design and operations of solar-powered aircraft. In order to demonstrate how these investigations could affect the viability of the aircraft missions, the necessary calculations and simulations are carried out considering the most

Digital Object Identifier 10.4316/AECE.2022.01006

impacting EPS constraints. In the context of this paper, a suggested design methodology is presented (Fig. 1) to properly develop separately each EPS unit (Power Regulation Unit, PV Panel, and Power Storage Unit) aiming to reduce the time and cost of the HAPS project. Based on this design process, the development of the EPS will follow sequential steps from analysis, sizing, design, implementation, and testing. As shown in Fig. 1, the feedback of certain steps are allowed for a possible adaptation of the design or parameters. This design process must carry on until reaching suitable characteristics of EPS main parts with some essential changes.

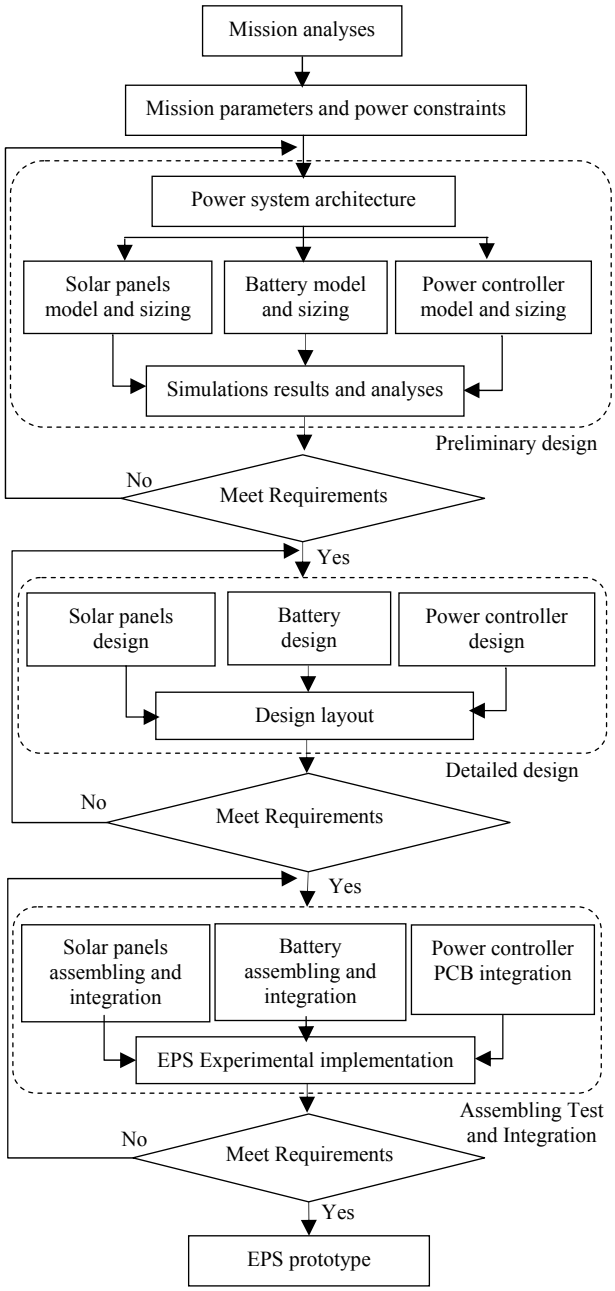

Figure 1. The suggested design methodology

Based on the flowchart above, the remaining part of this paper is organized as follows: Section 2 is dedicated to the mission parameters determination. In Section 3, the proposed EPS architecture is presented. The power budget calculation is described in Section 4. The power source sizing method is described in Section 5. In Section 6, the proposed Maximum Power Point Tracking (MPPT) technique based on Fuzzy Logic Controller (FLC) is illustrated. Then, in Section 7, the simulation results of the power control system and the HAPS energy balance are presented. Lastly, Section 8 discusses the conclusion and outcomes of the proposed study.

II. Mission Parameters Determination

The starting point for any subsystem design is the mission specifications and the spacecraft requirements, which define the purpose of the entire mission. The first step in designing the EPS is to define the power requirements based on the mission constraints. In this study, the HAPS mission is part of the Earth observation at 20 km altitude for 48 hours; the mission target is the city of Oran, located in the North-West of Algeria. Consequently, the HAPS must therefore carry all the necessary subsystems for this mission including the suitable payload. The mission parameter calculations presented in this section are performed using STK software.

On the earth's surface, the reached irradiance has various components: direct component coming directly from the Sun's surface, diffused component coming from all directions over the entire sky, and global component. The decrease in irradiance is due to several elements and factors in the stratosphere such as air molecules and the distance of sunlight to reach the earth's surface. The unit of Air Mass (AM) measures these factors, which is the ratio between the distance traveled by sunlight in the Earth's atmosphere and the distance it would travel if the sun were directly above. According to [22], the American Society for Testing and Materials (ASTM) provides measurement data, which reflect reference spectra with uniform wavelength intervals, under the influence of AM. This collected data is plotted, as shown in Fig. 2, where different AM conditions are displayed with their solar spectra for different wavelength values of light.

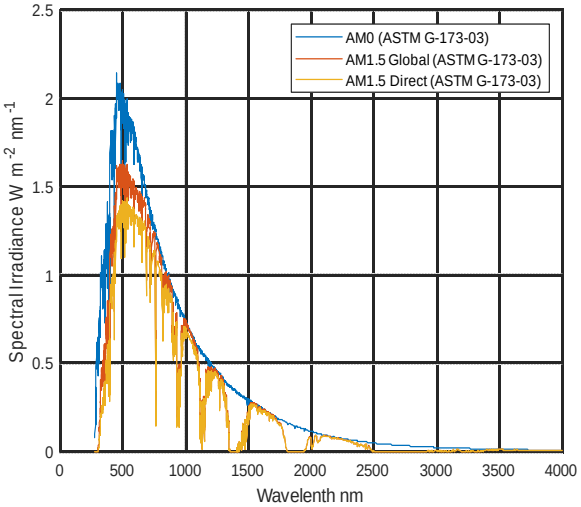

Figure 2. Solar irradiance spectrum above the atmosphere and at the surface

The AM1.5 has a significant effect on the collected energy by the photovoltaic system for HAPS. Indeed, the surface of the sun has about 6.33×107 W/m^2 of the radiation intensity, this intensity is reduced to 1000 W/m^2 after traveling from the sun to the stratospheric layer.

The energy delivered by the solar panels is strongly

influenced by the daylight duration and solar irradiance intensity, which are varying throughout the year. This will consequently lead the HAPS mission forecasting. For this reason, in this study, the flight is scheduled on two different dates (Best and Worst case) which are: May 22nd, 2022 (close to the summer solstice) and December 22nd, 2022 (Winter solstice), respectively. The mission parameters are resumed in Table I.

TABLE I. MISSION PARAMETERS

Place		Oran, Algeria
Flight Objective		Oran Imagine
Altitude		20 km
Flight Distance		3087.29 km
Flight Speed		72 km/h
Flight duration		34h 30mn
Flight Scenario n° 1	Launch date	May 22, 2022 @ 08 :00 AM
	Landing date	May 23, 2022 @ 18 :30 PM
Flight Scenario n° 2	Launch date	Dec 22, 2022 @ 08 :00 AM
	Landing date	Dec 23, 2022 @ 18 :30 PM

The instantaneous variation of the solar irradiance during one day is also a crucial parameter for energy generation, where, the duration, the start, and the end time of the mission require analysis for successful power management. In this paper, the HAPS mission is supposed to start in the morning to ensure that the solar panels will have sufficient time to charge the battery and to power all subsystems of the HAPS for a continuous flight. Regarding the landing process, it has to be done when the battery is sufficiently charged. The sunlight duration throughout the HAPS mission is calculated and shown in Table II for two mission scenarios' (Best and Worst case).

TABLE II. SUNLIGHT DURATION

Scenario n° 1 (Best Case)		
Start Time (UTCG)	**End Time (UTCG)**	**Duration (sec)**
22 May 2022 08:00:00.000	22 May 2022 19:26:50.914	41210.914
23 May 2022 04:34:43.208	23 May 2022 18:24:38.671	49795.46
Total Duration		**91006.377**
Scenario n° 2 (Worst Case)		
22 Dec 2022 08:00:00.000	22 Dec 2022 17:13:18.059	33198.059
23 Dec 2022 06:49:32.629	23 Dec 2022 17:15:06.057	37533.42
Total Duration		**70731.487**

III. PROPOSED POWER SYSTEM ARCHITECTURE

The proposed EPS architecture for the HAPS mission is presented in Fig. 3. One part of the harvested energy is transferred to the onboard payloads and subsystems; the other part is stored in the battery using the Battery Charge Regulator (BCR) for night flight. A Peak Power Tracker (PPT) circuit ensures the maximum power delivered by the solar panels.

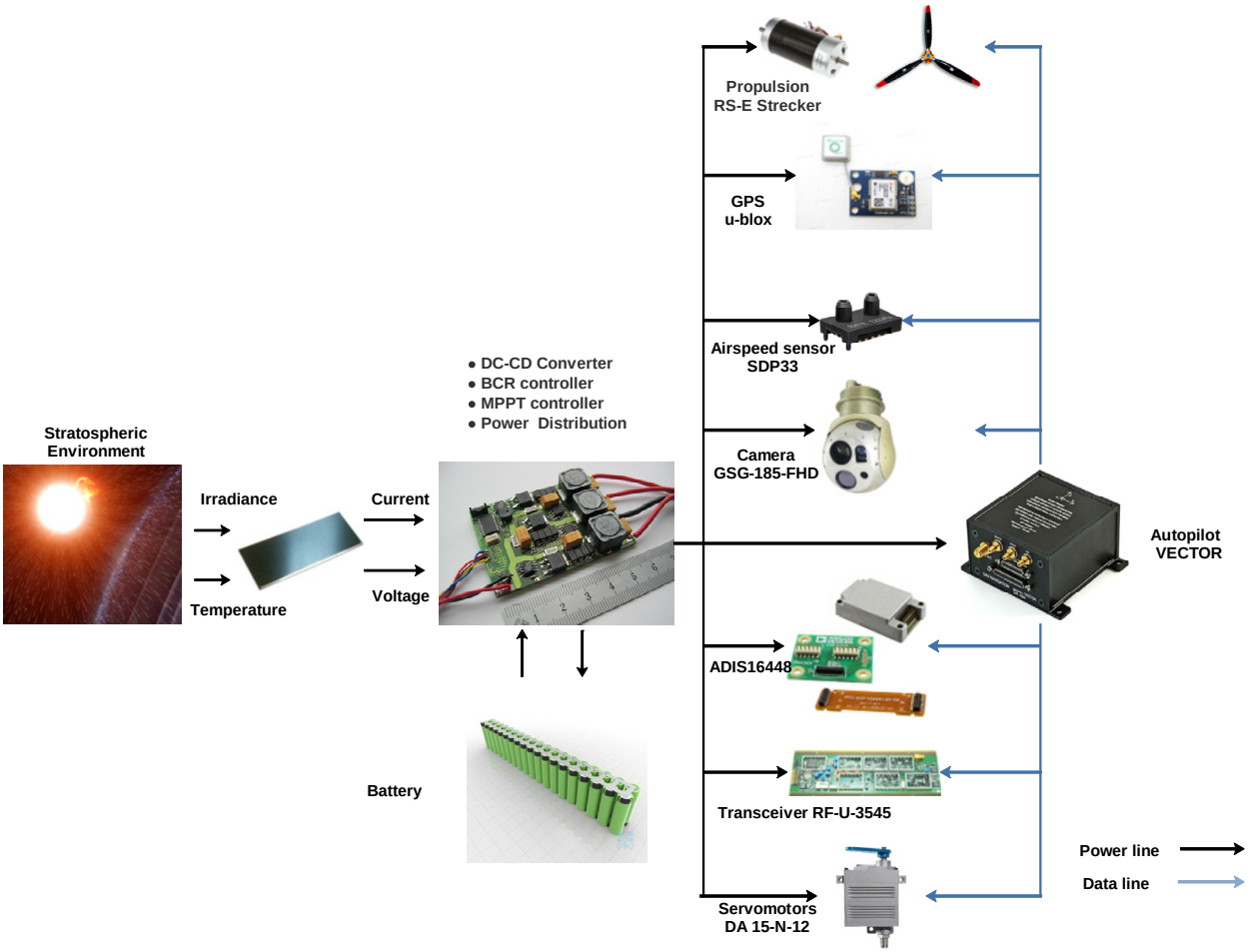

Figure 3. Proposed power system architecture for the HAPS

IV. POWER BUDGET

Once the mission requirements have been defined and the EPS architecture for HAPS is developed, the next step in the design process is to calculate the detailed power budget for all subsystems, where, the duty cycle of each equipment

(peak and quiescent power) should be defined. Furthermore, the calculated power budget of the HAPS is based on the maximum power consumption of its onboard equipment under worst-case conditions; a 30% margin is added to the total power consumption to consider any unexpected consumption excess, as suggested by [23]. The power budget calculation allows also the sizing of other components constituting the power system such as connectors, electrical cables, etc. The calculated power budget is then used to size the solar array and the battery capacity. The power dissipation may vary significantly during day and night, during the Beginning Of Life (BOL), and at the End Of Life (EOL), such variations must properly be taken into account. The power consumption of all subsystems constituting the HAPS are presented in Table III; the choice of these equipment is made carefully to fulfill the mission and also by reference to the manufacturer's reputation and flight heritage.

TABLE III. POWER BUDGET OF THE HAPS SUBSYSTEMS

Mode			**1**		**2**				**3**	
Description			**Take off**		**Nominal mode**				**Landing**	
Subsystems	**Components**	**Power (W)**	**Start at 8h:00**		**Day**		**Night**		**Start at 17h30**	
			Duration :1h		**Duration: 22h30mn**		**Duration:10h**		**Duration :1h**	
			Duty cycle (%)	**Power (W)**	**Duty cycle (%)**	**Power (W)**	**Duty cycle (%)**	**Power (W)**	**Duty cycle (%)**	**Power (W)**
Communications	X band	200	0	0	44.5	89	5	10	0	0
	RF-U-3545-TR-2	7.5	100	7.5	100	7.5	100	7.5	100	7.5
ADCS	ADIS16448	0.35	100	0.35	100	0.358	100	0.358	100	0.358
Autopilot	VECTOR	2.5	100	2.5	100	2.5	100	2.5	100	2.5
GPS	u-blox 6 GPS	0.5	100	0.5	100	0.5	100	0.5	100	0.5
payloads	Camera: GSG-185-FHD-XGA	60	100	60	100	60	20	12	100	60
Servomotors	DA 15-N-12-BLDC-32	53.2	100	53.2	100	53.2	100	53.2	100	53.2
Airspeed sensor	SDP33 sensirion	0.03	100	0.03	100	0.03	100	0.03	100	0.03
Propulsion	brushless DC motors	1600	100	1600	100	1600	12.5	200	100	1600
EPS (electronics)	MPPT, BCR, PDM	3	100	3	100	3	100	3	100	3
Total power (W)				1727.08		1816.08		289.088		1727.08
Margin (%)	30			518.12		544.82		86.72		518.12
Max power needed at EOL (W)				**2245.21**		**2360.91**		**375.81**		**2245.21**

V. POWER SOURCES SIZING

The sizing process is done in such a way that the battery is capable to ensure almost all the power required during takeoff, landing, and night time, where, the solar panel is capable of charging the battery during the daylight and ensuring the HAPS power required in the nominal mode operation.

A. Nominal Bus Voltage

The nominal bus voltage of the HAPS power system is fixed at 29V since the selected subsystems within this study have been previously designed to this voltage level. However, the choice of the bus voltage is basically a trade-off between the heritage of existing hardware, the availability and the reliability of circuit components, and overall system power losses.

B. Battery Sizing

The selected battery is provided by Amprius [24]; this battery, which is used in the famous Airbus HAPS (ZEPHYR) [25], has the best capacity/weight ratio on the market. However, the estimated bus voltage of the proposed EPS design varies between 24.75V and 39.6V depending on the battery State of Charge (SOC). The battery capacity is calculated according to the following Equation (1) for Depth of Discharge (DOD) of 60%.

$$\text{Battery capacity} = \frac{(\text{daynight power}) \text{ x} (\text{time in hours})}{(\text{battery discharge voltage}) \text{ x Battery DoD}} \quad (1)$$

$$\text{Battery capacity} = \frac{375,81 \text{ x } 10}{30 \text{ x } 0.60} \quad (2)$$

$$\textit{Battery capacity} = 208.78 \, Ah \quad (3)$$

C. Solar Panels Sizing and Realization

The maximum surface area, in which the solar panels are mounted, is imposed by the aerodynamic profile of the HAPS. The purpose of this sizing is to find out if this area is sufficient for all solar panels needed to power the HAPS and fully charge the battery. The proposed sizing process is based on the selected solar cell technology provided by "MicroLink Devices", already used on the ZEPHYR platform [25].

The solar panel sizing formula, given by Eq. (4), is related to the average power discharged during the night time (P_{night}) and the power returning the discharged energy and supplying all subsystems (P_{sun}) during the daylight. This formula also considers the PPT accuracy factor n_{tr}, the efficiency factor, n_{ppt}, of the PPT power converter electronics, and the battery Recharge Fraction (RF) measured in ampere-hours. The required solar array power at PPT input is given in Table IV, which is calculated based on Eq. (4):

$$P_{sa} = \frac{P_{sun} + P_{night} * RF}{n_{ppt} * n_{tr}} \tag{4}$$

where, the P_{sa} outcome power margin is up to 21%, which is acceptable regarding the design considerations.

TABLE IV. THE SOLAR ARRAY CALCULATION PARAMETERS

Parameters	Values
P_{sa}	2949.79 W
P_{sun}	2360.91 W
P_{night}	375.8 W
n_{tr}	0.99
n_{ppt}	0.95
RF	1.1

The solar array sizing is strongly influenced by the predicted solar array operational for the highest temperature at EOL, where the lowest voltage from the solar array can be achieved. Under these conditions, the solar array voltage must be equal to or exceed the maximum charge voltage of the battery, in addition to the voltage drop of any components between the solar array and the battery. The solar array voltage determines the number of solar cells that are required in series. The HAPS is deployed at 20km in the stratosphere, at this altitude, the temperature is almost stable and varies between – 2°C and 0°C [27]. Therefore, the hottest solar array temperature occurs at maximum solar intensity, which takes place when the Earth is closest to the sun (perihelion). In this study, the data provided by the manufacturer are already at the hottest temperature condition compared to the stratospheric temperature where the HAPS will be deployed. Otherwise, if the provided temperature data are lower than the estimated temperature when the HAPS is deployed, the following Eq. (5) must be applied.

$$V_{sa_{Ti}} = V_{mp} - \left[\frac{dV_{mp}}{dT} * (T_i - T_n) / 1000 \right] \tag{5}$$

where, T_i and T_n in (°C), are the i^{th} temperature and reference temperature given by the manufacturer, respectively; V_{saTi} is the solar array voltage at i^{th} measured temperature, and V_{mp} is the solar array voltage at maximum power measured at the reference temperature given by the manufacturer; dV_{mp}/dt is the voltage-temperature coefficient given in (mV/°C).

The solar array voltage can be calculated by Eq. (6) as the sum of the maximum battery charge voltage (V_B) and the different voltage drops considered in the design, namely: voltage drop across the PPT converter, $V_{ppt_{drop}}$, the voltage of blocking diodes, V_D, and the voltage drop across wiring between the battery and solar array, V_W.

$$V_{sa_{req}} = V_B + \left(V_{ppt_{drop}} + V_D + V_w \right) \tag{6}$$

The required minimum solar array output voltage (V_{sa}) at its maximum power point is given in Table V.

TABLE V. MINIMUM SOLAR ARRAY OUTPUT VOLTAGE CALCULATION PARAMETERS

Parameters	Values
V_{sa}	33 V
V_B	29 V
$V_{ppt_{drop}}$	3 V
V_D	0.7
V_W	0.3

The effective solar panels' area required is another key element in the sizing process, which is mainly affected by the power density (PD_{ref}) of the selected solar cells. Furthermore, it is mandatory to consider the Packing Factor (PF) of the solar panel (estimation of the spaces between cells, the stay-out areas for hinges, and other mechanical and electrical elements). Equation (7) is used for the calculation of the solar panels' effective areas;

$$Total\ Solar\ Array = \frac{P_{sa}}{PD_{ref} * PF} \tag{7}$$

MicroLink Devices is capable to provide solar panels with the power density of 250W/m², with a PF of 80%, where, the effective solar cell area required is then calculated by using Eq. (7):

$$Total\ Solar\ Array = \frac{2949.79}{250\ *0.8} = 14.74 m^2 \tag{8}$$

Note that the maximum surface of the HAPS, as imposed by the aerodynamic structural constraints, which can be covered by solar cells is 16 m².

The sizing results, presented in this section, stated that the solar panels' area of at least 16m² is sufficient to provide the minimum required energy. However, this sizing must be enhanced with the inclusion of the mission constraints.

VI. PROPOSED POWER CONTROL SYSTEM

In aerospace applications, a large number of power regulation techniques are used. These techniques can be divided into two main categories: PPT that operates between the solar panels and the main voltage bus, adjusting the solar panels' operation voltage to regulate its power; the Direct Energy Transfer (DET), placed in parallel between the solar panels and the main voltage bus diverting the current from the main bus to achieve the required voltage level.

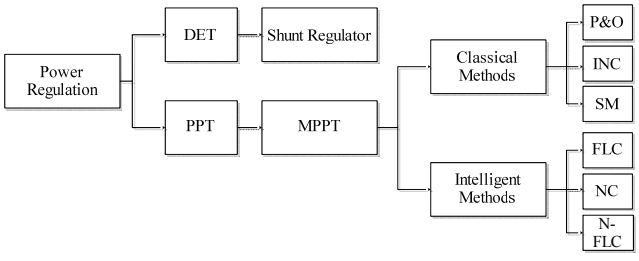

Figure 4. Power regulation topologies

After a detailed study of the main existing topologies presented in Fig. 4, the regulated PPT is selected for this

mission, which is most advantageous for those applications where the solar array I-V curve varies during the mission. The PPT is capable of continuously extracting the maximum power from the solar array by moving the solar operating voltage to the Maximum Power Point (MPP) voltage. However, to maintain the MPP operation in all environmental conditions (irradiance and temperature), it is only possible to act on the main voltage bus. The controlled variation of the voltage can be made through a DC-DC converter, while specific and well-defined algorithms guarantee automatic action on its duty cycle. The P&O method is the most widely used in photovoltaic systems [28-29] because of its simplicity and easy implementation. The operating principle of this method is to generate a periodic disturbance of the operating voltage and observe its effect on the output power.

Essentially, the HAPS's EPS is based on one of the techniques presented in Fig. 4, however, no study has revealed which MPPT algorithm is suitable for HAPS applications. In this paper, an improved Fuzzy Logic (FL) technique is proposed for the HAPS's EPS and then compared to the most used MPPT technique (P&O), in terms of performance and stability.

The design of the FL Controller (FLC) varies according to the choice of input and output variables, which introduces different effects on the MPPT process. The output variable is usually the duty cycle of the DC-DC converter. However, the input variables and their specifications are not always the same. The most commonly used input variables for MPPT algorithms are based on the electrical characteristics of the PV system. [31] used the rate of change in photovoltaic system output power and the rate of change in photovoltaic system terminal voltage (*dP/dt, dV/dt*) as inputs variables. [32] used the errors *E(P,V)* and the error variation *ΔE* of the PV system. Other studies selected as input variables the power and voltage variations (*ΔP*, *ΔV*) [33]. So far, despite all these combinations, no work has selected the duty cycle variation as a fuzzy input variable. Therefore, in this study, a novel efficient FLC-MPPT technique is proposed to automatically and intelligently adjust the duty cycle as well as improve the efficiency of the PV system.

The proposed FLC has two inputs and one output. The input variables are: the mean of Duty Cycle (t) and the variation of the PV system power; the output is the Duty cycle, with

$$Mean(DutyCycle(t)) = \frac{1}{T}\int_{t-T}^{t} DutyCycle(t).dt \qquad (9)$$

Fig. 5 shows the flowchart of the proposed fuzzy controller calculation process.

The fuzzification strategy is chosen by defining the membership functions forms and their arrangement on the universe of discourse. Several membership functions can be defined: triangular, trapezoid, singleton, sigmoid, Gaussian, etc. According to the experimental results conducted in [34], the three membership functions (triangular, trapezoid, and Gaussian) provide similar good results, hence, the triangular one is the most used due to its smooth implementation process [31-33].

The fuzzy rules are defined from the description of the system to be controlled according to the linguistic variables and the input/output membership functions. The complete base of the proposed FLC rules is presented in Table VI, with a total of 25 implemented fuzzy rules.

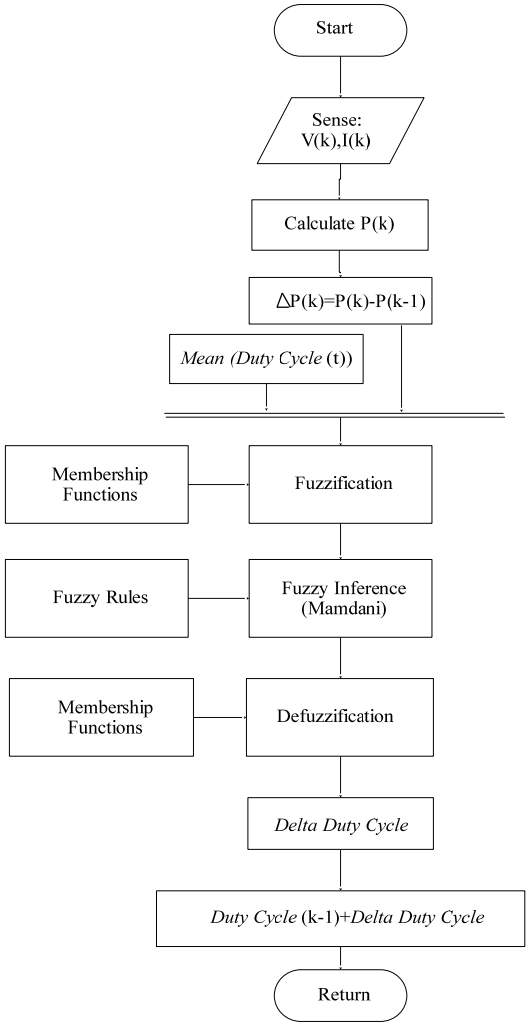

Figure 5. Proposed MPPT based on FLC

TABLE VI. COMPLETE RULE BASE FOR THE PROPOSED FLC.

		ΔP				
		NG	***NM***	***C***	***PM***	***PG***
Mean D_{in}	***VS***	*CO*	*CO*	*CO*	*P*	*PM*
	SM	*N*	*N*	*CO*	*P*	*PM*
	M	*NM*	*N*	*CO*	*P*	*PM*
	FA	*NM*	*N*	*CO*	*CO*	*P*
	VF	*NM*	*N*	*CO*	*CO*	*CO*

Fig. 6 shows the behavior of the output ΔD_{out} of the FLC compared to the two inputs variations.

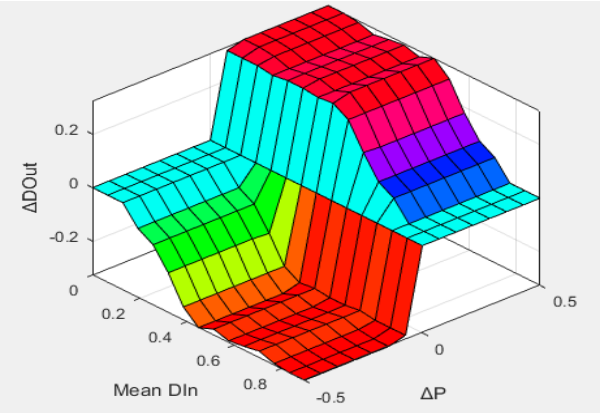

Figure 6. Variation of the ΔD_{out} at instant *K* as a function of the variation of the inputs *ΔP* and *Mean* D_{in}

VII. Simulations Results

A. Proposed Power Control

In order to demonstrate the efficiency of the proposed FLC strategy, a comparison of results obtained by simulations of the power generated by part of the HAPS solar panels is carried out using Matlab/Simulink (Fig. 7 and Fig. 8).

It can be observed that, during the irradiance and the temperature changes, the obtained powers from the two MPPT control methods FLC and P&O have effectively tracked their MPP. However, the proposed FLC method provides a slightly higher amount of power with less oscillation compared to the second MPPT technique. This allows more stable voltage bus which increases (according to ECSS standards [35]) the lifespan of the electrical subsystems hence the availability of the HAPS mission.

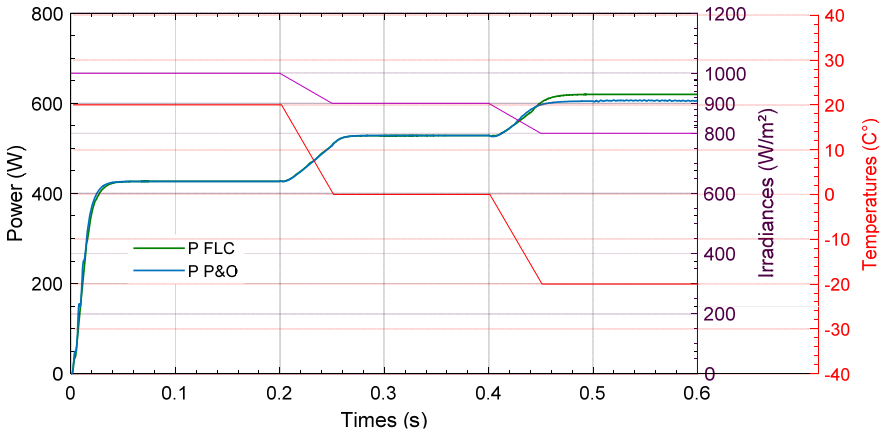

Figure 7. Output Powers obtained by the two MPPT algorithms, P&O and FLC, for different irradiance and temperature values.

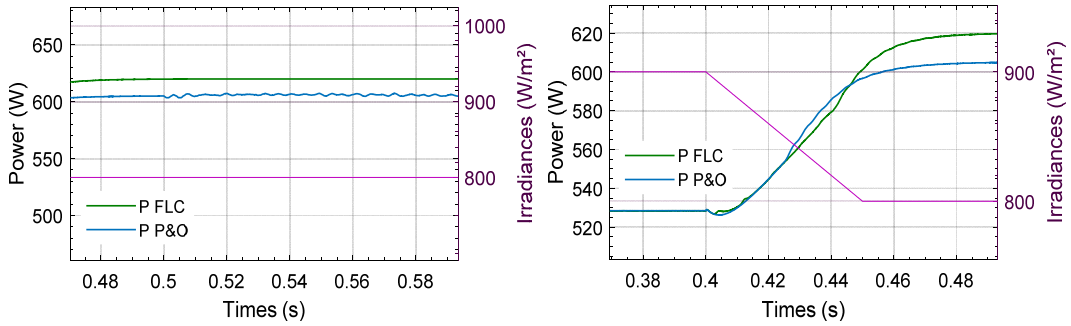

Figure 8. Zoom of the output powers: (a) at 900W/m² & 0 C°; (b) during conditions changes from 900 W/m² & 0 C° to 800 W/m² & -20 C°.

B. Power Balance Analysis

The mission target of the HAPS is Oran for Earth observation, at an altitude of 20km with a speed of 72km/h. In this section, the simulations of the instantaneous, harvested power, consumed power, and the battery capacity during the entire mission, are done with the consideration of:

- The shape of the top face of the HAPS, where the solar panels are mounted;
- The itinerary and maneuvers of the HAPS during its mission;
- The geographical location, period, and duration of the HAPS mission.

The maximum instantaneous electrical power that can be generated by each solar panel are shown in Fig. 9 and Fig. 10, where, the calculation is done according to the following formula:

$$P = C_s * I_s * n * Aeff \quad (10)$$

with:

n - efficiency of the selected solar cells:

I_s - solar intensity ranges from umbra (0), through penumbra ($0 < i < 1$), to full sunlight (1);

A_{eff} - effective area (m²);

C_s - solar irradiance (W/m²).

It is obvious that the angles between the sun irradiances and the HAPS solar panels vary constantly depending on the mission profile. This causes considerable variations in the power generated by each solar panel. On the other hand, the simulations show that the average power produced during scenario n° 2 (worst case, Fig. 10) has lost an amount of 1483 W compared to that produced in scenario n° 1 (Best case, Fig. 9). Since, in this period (scenario n° 2), the HAPS solar panels receive lower solar intensity in the shortest daylight in the year (December 22nd: Winter Solstice). This explains clearly the importance of choosing the date and duration of the mission in terms of energy. In addition, such a power difference (1483 W) has definitely a very significant financial impact regarding the cost of the HAPS's solar panels.

Figure. 9 and Fig. 10 show also that solar panels 1 and 2 are the most influenced by the trajectory and flight maneuvers. Whereas, the solar panel 3, mounted on the upper face, is always parallel to the plane of the trajectory and influenced only by the HAPS's flight maneuvers. This is illustrated more clearly in the simulation on May 23rd and December 22nd between 7: 26 AM and 8: 31 AM. Conversely, when the sun vector is not facing the HAPS trajectory, the solar panel 2 will produce the most effective power.

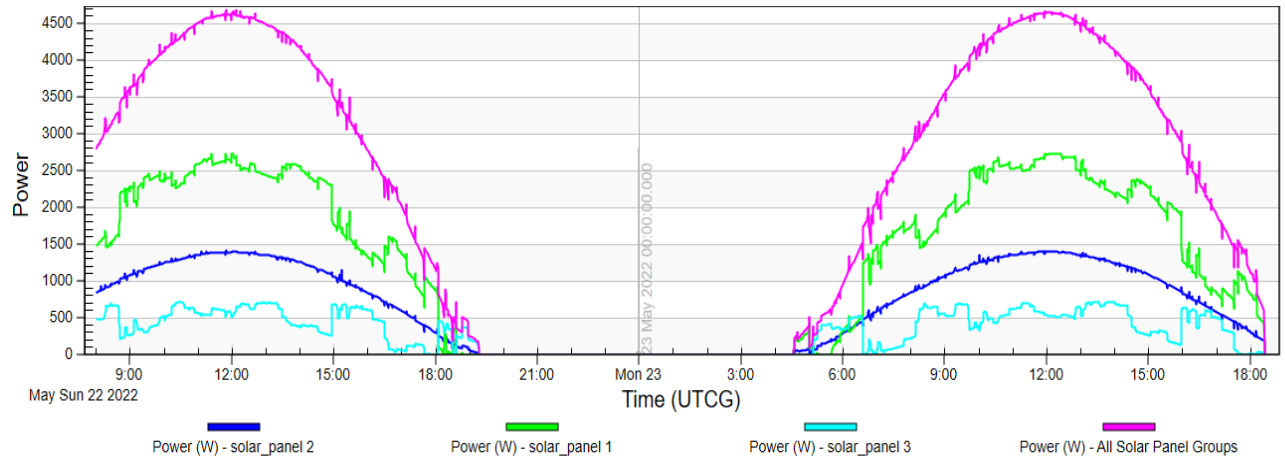

Figure 9. Solar panels power (Best case)

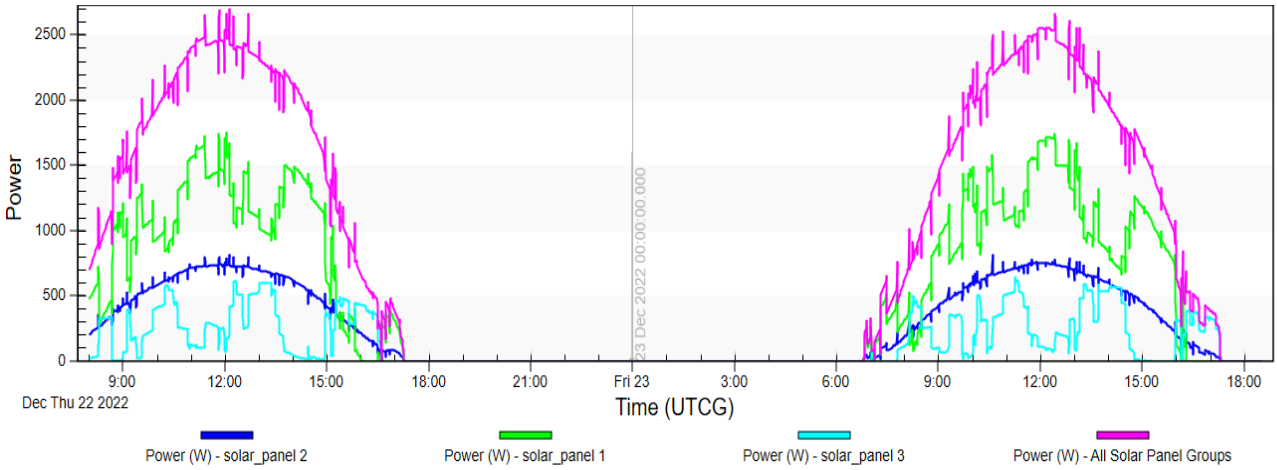

Figure 10. Solar panels power (Worst case)

This can be observed by the simulation results generated for the dates of May 22nd from 4:43 PM to 5:00 PM (Fig. 9), and on Dec. 22nd from 09:43 AM to 12:05 AM. (Fig. 10). Therefore, it is necessary to make sure that the largest solar panel is well facing the solar irradiance as long as possible when defining the itinerary of the HAPS.

Fig. 9 and Fig. 10 show also that the electrical power produced depends on the maneuvers executed by the HAPS to follow its trajectory, where it must tilt to be able to turn; (eg. May 22nd at 9:39 AM, May 22nd, 2022 at 12:05 AM, December 21st, 2022 at 2:37 PM etc.). These tilts can be in favor or restricted for power production, which depends on the direction of the inclinations of the HAPS regarding the sun vector. Therefore, during daylight operations, it is recommended to minimize the duration and number of any undesirable maneuvers as much as possible. In the second part of the simulation, a comparison between the estimated power generation and consumption is performed. The power balance of the HAPS during the mission for the two distinct scenarios: The Best case and the Worst case, is illustrated in Fig. 11 and Fig. 12. The different states of the power consumption are described in Table VII.

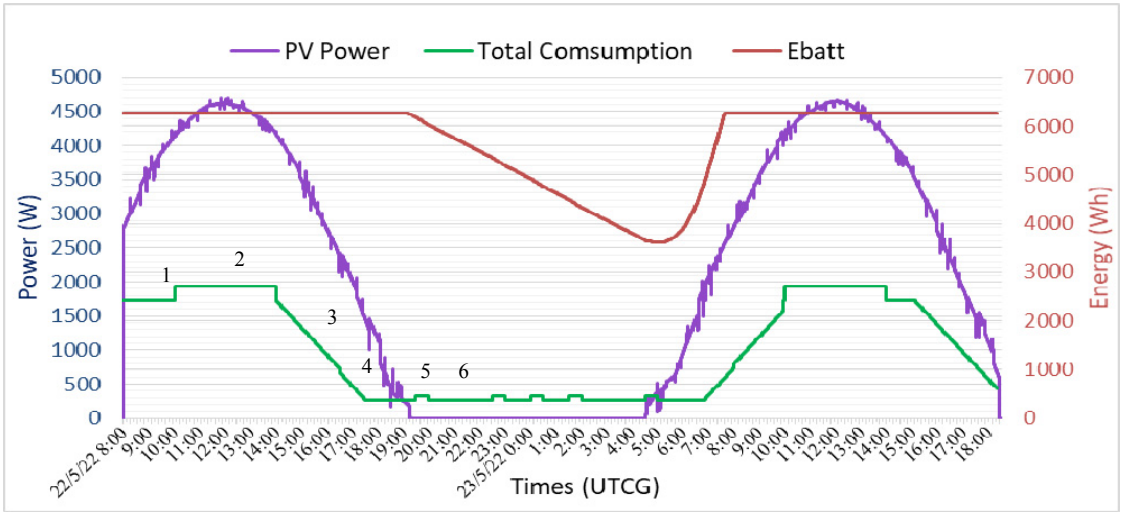

Figure 11. HAPS powers simulation during 34h (Best case)

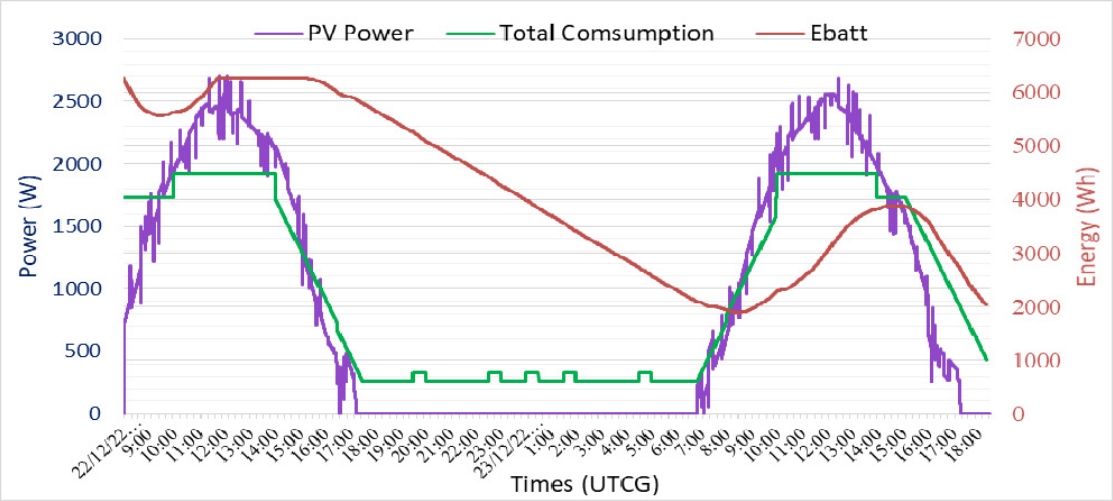

Figure 12. HAPS powers simulation during 34h (Worst case).

TABLE VII. DESCRIPTION OF THE HAPS POWER CONSUMPTION

States N°	Descriptions
1	All subsystems are ON except the X Band is OFF
2	All subsystems are ON
3	State 1 + The propellers are reducing their speeds and consequently the power consumption
4	State 3 + Camera OFF
5	State 1 + The propellers are at the minimum permitted speed
6	State 5 + Camera OFF

The results obtained for both cases (Best and Worst) confirm that the EPS satisfied the energy needed by the HAPS during the entire mission, which validates the power sources sizing technique.

Figure 11 presents the most favorable scenario, where, at this period of the year, the intensity and duration of the daylight are at their maximum, the solar panels generate then enough energy to fully charge the battery and ensure the energy requirements for all subsystems. On the other hand, the battery is capable to provide the necessary energy during the night with 42% of DoD. This does not ensure only a successful mission of the HAPS, but can also extend the flight duration to several weeks.

Figure 12 illustrates the worst scenario, where, the intensity and the daylight period are very low in this period compared to the previous one. Whereas, the solar panels can hardly provide sufficient energy for the subsystems and are not able to fully charge the battery. In this worst case, the mission lifespan cannot exceed 48 hours. During this long nighttime, the battery can provide power to the HAPS but with a very high DoD (70%), which can cause serious damage to the battery lifecycle.

The analyses results have been revealed that HAPS power generation is dependent on mission parameters (locations, mission times, and itinerary), and explain clearly the important consideration of the mission's date. Accordingly, from the analysis of the power balance, it has been affirmed through this study, that the aerodynamic envelope of the HAPS must be evaluated as a constraint to optimize the EPS architecture of the HAPS.

VIII. CONCLUSION

In this paper, the topology proposal of the Electrical Power System (EPS) for a High-Altitude Pseudo-Satellite (HAPS) is investigated within the framework of an Earth observation mission. The proposed design method of the EPS is initiated by the mission analysis phase of the HAPS project, to determine the mission parameters and requirements. Accordingly, the suggested EPS architecture is established. Then, the power balance is estimated for the different mission scenarios, where the electrical power consumption of all the equipment constituting the HAPS has been considered.

The proposed power control technique of the HAPS is presented. According to the comparative study of different MPPT methods, which is approved by the simulation results, the output power performances obtained by the proposed FLC-based MPPT methods is better than that of the conventional P&O-based MPPT method.

This paper also presents an appropriate suggested sizing technique for the HAPS power sources. As a result, from the analysis of the energy balance, it has been affirmed through this study, that the HAPS mission can be successful by using the suggested sizing techniques and design methodology.

REFERENCES

[1] J. Gonzalo, D. Lopez, D. Dominguez, A. Garcia, and A. Escapa, "On the capabilities and limitations of high altitude pseudo-satellites," Progress in Aerospace Sciences, vol. 98, pp. 37-56, 2018. doi:10.1016/j.paerosci.2018.03.006

[2] T. Fehr, M. Davidson, A. Ciccolella, and J. Lizarraga Cubillos, "High-altitude pseudo-satellites-an emerging tool in support of earth observation satellite development, calibration/validation and

applications," in EGU General Assembly Conference Abstracts, 2018, pp. 17497
[3] M. M. Fladeland, "Recent advances in high altitude pseudosatellites (HAPS) and potential roles in future earth observing systems," 2019
[4] R. Müller, J. J. Kiam, and F. Mothes, "Multiphysical simulation of a semi-autonomous solar powered high altitude pseudo-satellite," in 2018 IEEE Aerospace Conference, 2018, pp. 1-16
[5] F. Akram, H. Khan, T. Shams, and D. Mavris, "Design space optimisation of an unmanned aerial vehicle submerged inlet through the formulation of a data-fusion-based hybrid model," The Aeronautical Journal, pp. 1-18
[6] R. Dancila and R. Botez, "New flight trajectory optimisation method using genetic algorithms," The Aeronautical Journal, vol. 125, pp. 618-671, 2021. doi:10.1017/aer.2020.138
[7] A. Klockner, Behavior trees for mission management of high-altitude pseudo-satellites: Dr. Hut, 2016
[8] B. Kirsch and O. Montagnier, "Towards the advent of high□altitude pseudo-satellites (HAPS)," Disruptive Technology and Defence Innovation Ecosystems, vol. 5, pp. 181-201, 2019. doi:10.1002/9781119644569.ch9
[9] T. Ma, Y. Liu, D. Yang, Z. Zhang, X. Wang, and S. Hao, "Research on the design of smart morphing long-endurance UAVs," The Aeronautical Journal, vol. 125, pp. 22-41, 2021. doi:10.1017/aer.2020.82
[10] A. Alsahlani, L. Johnston, and P. Atcliffe, "Design of a high altitude long endurance flying-wing solar-powered unmanned air vehicle," Progress in Flight Physics, vol. 9, pp. 3-24, 2017. doi:10.1051/eucass/201609003
[11] W. H. Phillips, "Some design considerations for solar-powered aircraft," National Aeronautics and Space Administration, Hampton, VA (USA). Langley, 1980
[12] D. Park, Y. Lee, T. Cho, and C. Kim, "Design and performance evaluation of propeller for solar-powered high-altitude long-endurance unmanned aerial vehicle," International Journal of Aerospace Engineering, vol. 2018, 2018. doi:10.1155/2018/5782017
[13] P. Oettershagen, A. Melzer, T. Mantel, K. Rudin, T. Stastny, B. Wawrzacz, T. Hinzmann, S. Leutenegger, K. Alexis, and R. Siegwart, "Design of small hand-launched solar-powered UAVs: From concept study to a multi-day world endurance record flight," Journal of Field Robotics, vol. 34, pp. 1352-1377, 2017. doi:10.1002/rob.21717
[14] B. Kranjec, S. Sladic, W. Giernacki, and N. Bulic, "PV system design and flight efficiency considerations for fixed-wing radio-controlled aircraft-A case study," Energies, vol. 11, p. 2648, 2018. doi:10.3390/en11102648
[15] M. Brizon, "Solar energy generation model for high altitude long endurance platforms," ed, 2015
[16] T. Smith, M. Trancossi, D. Vucinic, C. Bingham, and P. Stewart, "Primary and albedo solar energy sources for high altitude persistent air vehicle operation," Energies, vol. 10, pp. 573, 2017. doi:10.3390/en10040573
[17] D. Liviu, C. J. Ileana, and G. T. Lucian, "Energy conversion systems for high altitude pseudo-satellites," International Multidisciplinary Scientific GeoConference: SGEM: Surveying Geology & mining Ecology Management, vol. 17, pp. 223-230, 2017
[18] J. Barbé, A. Pockett, V. Stoichkov, D. Hughes, H. K. H. Lee, M. Carnie, T. Watson, and W. C. Tsoi, "In situ investigation of perovskite solar cells' efficiency and stability in a mimic stratospheric environment for high-altitude pseudo-satellites," Journal of Materials Chemistry C, 2020. doi:10.1039/C9TC04984C
[19] J.-I. Corcau, L. Dinca, M. Culcer, and M. Gheorghe, "Modeling and Simulation of Hybrid Power Source for Pseudo-Satellites," in 2018 International Symposium on Power Electronics, Electrical Drives, Automation and Motion (SPEEDAM), 2018, pp. 1055-1060. doi:10.1109/SPEEDAM.2018.8445208
[20] K. Shin, H. Hwang, and J. Ahn, "Mission analysis of solar UAV for high-altitude long-endurance flight," Journal of Aerospace Engineering, vol. 31, pp. 04018010, 2018. doi:10.1061/(ASCE)AS.1943-5525.0000832
[21] S. C. Arum, D. Grace, P. D. Mitchell, M. D. Zakaria, and N. Morozs, "Energy management of solar-powered aircraft-based high altitude platform for wireless communications," Electronics, vol. 9, p. 179, 2020. doi:10.3390/electronics9010179
[22] W. J. Larson and J. R. Wertz, "Space mission analysis and design," Torrance, CA (United States); Microcosm, Inc.1992. doi:10.1007/978-94-011-2692-2
[23] J. R. Wertz, and W. J. Larson, Space Mission Analysis and Design, 3rd ed., pp. 316, El Segundo, California, Microcosm Press and Kluwer Academic, 1999.
[24] G. Warwick, "Record-breaking Zephyr's battery holds eVTOL potential: Amprius cells helped power Zephyr stratospheric UAV; company's current focus is on the aerospace market and high-performance UAVs," Aviation Week & Space Technology, 2019
[25] A. Defence, "Space,"Zephyr, the High Altitude Pseudo-Satellite," 2017
[26] W. J. Larson and J. R. Wertz, "Space mission analysis and design," Torrance, CA (United States); Microcosm, Inc., 1992. doi:10.1007/978-94-011-2692-2
[27] A. C. Maycock, W. J. Randel, A. K. Steiner, A. Y. Karpechko, J. Christy, R. Saunders, D. W. Thompson, C. Z. Zou, A. Chrysanthou, and N. Luke Abraham, "Revisiting the mystery of recent stratospheric temperature trends," Geophysical research letters, vol. 45, pp. 9919-9933, 2018. doi:10.1029/2018GL078035
[28] A. Belkaid, I. Colak, and K. Kayisli, "Implementation of a modified P&O-MPPT algorithm adapted for varying solar radiation conditions," Electrical Engineering, vol. 99, pp. 839-846, 2017. doi:10.1007/s00202-016-0457-3
[29] K. A. Mohamed, M. Zakareya, K. H. Youssef, and H. A. Khater, "Improved perturb and observe maximum peak power tracking for solar satellite systems," in IOP Conference Series: Materials Science and Engineering, 2019, pp. 012091. doi:10.1088/1757-899X/610/1/012091
[30] H. Taha, R. Mostafa, U. Abouzayed, and F. Eltohamy, "Design and Implementation of PV MPPT Controller based on modified P&O algorithm using FPGA for satellite systems," in 2018 13th International Conference on Computer Engineering and Systems (ICCES), 2018, pp. 524-529. doi:10.1109/ICCES.2018.8639231
[31] N. Altin, "Interval type-2 fuzzy logic controller based maximum power point tracking in photovoltaic systems," Advances in Electrical and Computer Engineering, vol. 13, pp. 65-71, 2013. doi:10.4316/AECE.2013.03011
[32] D. Petreus, D. Moga, A. Rusu, T. Patarau, and M. Munteanu, "Photovoltaic system with smart tracking of the optimal working point," Advances in Electrical and Computer Engineering, vol. 10, pp. 40-47, 2010. doi:10.4316/aece.2010.03007
[33] A. Al-Gizi, S. Al-Chlaihawi, M. Louzazni, and A. Craciunescu, "Genetically optimization of an asymmetrical fuzzy logic based photovoltaic maximum power point tracking controller," Advances in Electrical and Computer Engineering, vol. 17, pp. 69-76, 2017. doi:10.4316/AECE.2017.04009
[34] R. Rahim, "Comparative analysis of membership function on Mamdani fuzzy inference system for decision making," in Journal of Physics Conference Series, 2017, p. 012029. doi:10.1088/1742-6596/930/1/012029
[35] ESA, "Space engineering," in Electrical and electronic, ed. Noordwijk, The Netherlands: ESA Requirements and Standards Division